

NACA RM A53117

0220

TECH LIBRARY KAFB, NM  
0143352

NACA

# RESEARCH MEMORANDUM

A STUDY OF THE EFFECTS OF BODY SHAPE ON THE  
VORTEX WAKES OF INCLINED BODIES

AT A MACH NUMBER OF 2

By Forrest E. Gowen and Edward W. Perkins

Ames Aeronautical Laboratory  
Moffett Field, Calif.

Classification cancelled (or changed to *UNCLASSIFIED*)

By Authority of *NASA Tech Rep Announcement #197*  
(OFFICER AUTHORIZED TO CHANGE)

By *J. C. Stutz*

GRADE OF OFFICER MAKING CHANGE)

DATE

CLASSIFIED DOCUMENT

NATIONAL ADVISORY COMMITTEE  
FOR AERONAUTICS

WASHINGTON

December 1, 1953



## NATIONAL ADVISORY COMMITTEE FOR AERONAUTICS

RESEARCH MEMORANDUM

## A STUDY OF THE EFFECTS OF BODY SHAPE ON THE

## VORTEX WAKES OF INCLINED BODIES

## AT A MACH NUMBER OF 2

By Forrest E. Gowen and Edward W. Perkins

## SUMMARY

Visual-flow studies were made of the behavior of the vortices which form in the separated flow region in the lee of an inclined body of revolution. These studies were conducted at a Mach number of 1.98 in the range of Reynolds numbers (based on body diameter) from 0.1 million to 0.8 million. It was noted that, in general, the configuration of vortices in the wake could be changed by varying the position of the crossflow separation lines along the sides of the body. It was found that the angle of attack at which the vortex wake became unsteady could be increased by reducing the nose fineness ratio, or, for a given nose fineness ratio, by increasing the bluntness of the profile. For slender nose shapes (fineness ratios of the order of 6 and greater), an increase in Reynolds number resulted in a decrease in the angle of attack at which asymmetry and subsequent unsteadiness in the wake flow occurred. For low fineness-ratio bodies (fineness ratios of the order of 3 and less), changes in Reynolds number had little effect on the wake vortex configuration. The lift, drag, and pitching-moment characteristics of a  $5^\circ$  cone were negligibly affected by changing the steady wake vortex configuration from symmetric to asymmetric.

## INTRODUCTION

The maneuverability requirements for high-speed, high-altitude missiles have led to the need for knowledge of the aerodynamics of bodies at large angles of attack. Studies of the angle-of-attack characteristics of a number of bodies have revealed that the flow on the lee side of these bodies is characterized by a vortex system. It has been shown in reference 1 that as the angle of attack is increased the vortex system changes from a steady symmetric pair to a steady asymmetric configuration of two or more vortices and, finally, at large angles of

attack, to an unsteady asymmetric arrangement. It is evident that these vortices can affect the stability of body-tail configurations if the vortex paths pass near the tail surfaces. If this vortex flow is steady, there should be no difficulty in the calculation of the induced effects on the tail surfaces, provided that the strengths and positions of the vortices are known. However, if the wake vortex flow is unsteady, then large and erratic fluctuations of the forces on the tail surfaces such as those discussed in references 2, 3, and 4 may occur, and it may be impossible to control the roll attitude of a missile subjected to this dynamic condition.

The emphasis of the present investigation has been placed upon a study of factors which affect the onset of unsteady wake flow since greater control difficulties are associated with the unsteady vortex wake than with either of the other wake configurations. It is realized that for full-scale vehicles in flight there exists the possibility of coupling between the shedding of the wake vortices and the movement of the aircraft. Hence, the results of a wind-tunnel investigation using a model, the movement of which is restrained by its mounting system, may not be directly applicable to full-scale vehicles. However, the effects on the wake vortex configuration of certain variables such as model geometry and Reynolds number may indicate significant trends. It has been previously shown in references 2 and 3 that both the vortex configuration in the lee of a body and the magnitude of the rolling moment accompanying an asymmetry in the vortex pattern were altered by changing the nose shape from conical to ogival. In order to investigate further the effects on the wake vortex pattern of changing the nose shape as well as the effects of other variables, such as afterbody shape, separation-fixing devices, and Reynolds number, the present investigation was undertaken.

## APPARATUS AND TESTS

### Wind Tunnel

The investigation was conducted in the Ames 1- by 3-foot supersonic wind tunnel No. 1, which is a closed-return, continuous-operation, variable-pressure tunnel with a maximum operating Mach number of 2.2. The nozzle of this tunnel is equipped with flexible top and bottom plates for varying the test-section Mach number. The tunnel auxiliary equipment includes a standard schlieren optical system and a vapor-screen apparatus. The latter is used for visualizing flow phenomena in planes perpendicular to the tunnel axis. (See refs. 1 and 4.) This vapor-screen apparatus is illustrated schematically in figure 1. Flow disturbances such as the vortices in the body wake and the conical shock wave from the nose of the body result in variations of the intensity of the scattered light in the plane of the vapor screen. These variations

in intensity can be observed and photographed. (The intersection of the Mach cone and the light plane is called Mach circle in fig. 1.) Most of the vapor-screen photographs included in this report were taken from a vantage point similar to that for figure 1 with the plane of the vapor screen near the base of the model. The photographs include only the portion of the flow field indicated in the figure.

### Models

Sketches and pertinent dimensions of all models are shown in figure 2. The first group of models (models 1-A through 12-B in fig. 2(a)) was used to study the effects of body shape on the wake vortex pattern. The model designations for this group include a number and a letter to identify the nose and afterbody, respectively. A second group of models was used to study the effects of afterbody expansion on the wake vortices. This group of models consisted of the triangular-plan-form wing models shown in figure 2(b) and the conical-afterbody models (models 7-A, 7-E, and 7-F) shown in figure 2(a). The effectiveness of various methods of stabilizing the crossflow wake at large angles of attack by providing sharp edges to fix the crossflow separation lines was studied by the use of the models shown in both figures 2(b) and 2(c). Two models with parabolic-arc profiles (fig. 2(d)) were also tested. One of these latter models was constructed with a nose spike in order to assess the effects of such a device on the wake vortices.

### Test Procedure

Vapor-screen photographs were taken for each model throughout an angle-of-attack range of  $0^\circ$  to about  $35^\circ$ . Certain of the models were tested at various roll angles to determine the effects of rotational asymmetry of the model on the vortex configuration. A Reynolds number variation from about 0.1 million to 0.8 million, based on free-stream conditions and maximum body diameter, was obtained by changing the tunnel total pressure.

In addition to the visual-flow study, measurements of the lift, drag, and pitching moment were made on a sharp  $5^\circ$  cone and then on a  $5^\circ$  cone which had a small tip modification sufficient to change the configuration of vortices in the wake.

## RESULTS AND DISCUSSION

### General Considerations

The wake vortex patterns on the lee side of lifting bodies fall into three categories; namely, a steady symmetric pair, a steady asymmetric configuration of two or more vortices, and an unsteady configuration of two or more vortices. For most models the steady symmetric pair of vortices, such as illustrated in figure 3(a), is observed in the low angle-of-attack range (angles of attack less than about  $15^\circ$ ). A steady asymmetric configuration, figure 3(b), is found in the intermediate angle-of-attack range (angles of attack between about  $15^\circ$  and  $28^\circ$ ), and the unsteady configuration is found at large angles of attack. The angle-of-attack range for which any particular vortex pattern exists depends upon a number of factors such as model geometry and Reynolds number. The present investigation is concerned primarily with the effects of these two factors on the angle of attack at which the unsteady vortex wake occurs. The results of this study are presented in the following discussion.

### Effects of Body Expansion

The analogy between the development with time of the flow about a two-dimensional circular cylinder impulsively set in motion from rest and the development with distance along the body of the crossflow about an inclined body has been pointed out in reference 1. This analogy suggests that if the body is designed with a large rate of increase of body cross-sectional area with distance along the body, both the symmetry and stability of the vortex pattern might be retained to large angles of attack. In order to investigate the effects on the wake vortex configuration of various rates in increase in body cross-sectional area, a series of cones, cone-cylinders, and other simple models were tested. The results of these tests will be considered in two parts: the expansion of the body nose, and expansion of the afterbody.

Expansion of the body nose.— The results of the tests with cones and cone-cylinders are presented in figure 4(a) in which the angle of attack at which unsteadiness in the crossflow first appeared is plotted as a function of nose apex angle. In this figure the plotted position of each symbol designates the lowest angle of attack at which wake unsteadiness was observed for the cone. In order to denote that unsteadiness in the wake was not observed within the angle-of-attack range of the tests for certain of the models, an arrow has been attached to the symbol and the symbol has been plotted at the maximum angle of attack of the tests. The curve drawn through the symbols thus indicates

an approximate division line between the region for steady wake flow and the region for unsteady wake flow.<sup>1</sup> This curve shows that an increase in the cone apex angle resulted in an increase in the angle of attack at which wake unsteadiness first occurred. Although the fairing of the experimental curve for angles of attack greater than  $30^\circ$  may appear somewhat arbitrary, it is based upon a number of observations of similar wakes and, in addition, on the following evidence. The data for the  $19^\circ$  and  $30^\circ$  apex angle cones (models 2-B and 1-A, respectively) indicate that at the maximum angles of attack for these two models ( $35^\circ$  and  $40^\circ$ , respectively) no unsteadiness in the wake flow occurred at a Reynolds number of 0.35 million. However, when the Reynolds number for the  $19^\circ$  cone was increased to 0.85 million, the wake became unsteady at an angle of attack of about  $33^\circ$ . Comparison of the corresponding vapor-screen photographs indicated that the wake flow for the test at the lower Reynolds number would probably have been unsteady at an angle of attack about  $2^\circ$  to  $4^\circ$  above the maximum available for this model. Therefore, the experimental curve has been faired accordingly. The second curve included in figure 4(a) was obtained from reference 5 and shows the theoretical variation with apex angle of the smallest angle of attack at which the laminar crossflow boundary layer separates with the presumed formation of wake vortices. It is apparent from the trends of the two curves in figure 4(a) that increasing the apex angles of cones and conical-nosed bodies (i.e., increasing the longitudinal rate of growth of the body cross section) increases both the angle of attack for the initial formation of the crossflow vortices and the angle of attack at which the vortex flow becomes unsteady. For a particular cone at the test Reynolds number of figure 4(a), the lowest angle of attack at which the vortex flow became unsteady was about five times the angle of attack at which the boundary layer theoretically separates.

The results for conical-nosed bodies of revolution have indicated that the apex angle is a dominant factor in determining the nature of the wake vortex pattern. One might also reason that for planar bodies such as triangular-plan-form wings the apex angle might also have an important effect, and comparison of the wake flow for a body of revolution, and a wing of similar plan-form apex angle would be of interest. Hence, a triangular-plan-form wing-body combination with a  $12^\circ$  apex angle (model 15) and an  $11\text{-}1/2^\circ$  apex angle cone-cylinder (model 3-C) were tested with similar ambient test conditions throughout the angle-of-attack range. For both models in the low angle-of-attack range, the vortex patterns were observed to be both steady and symmetric. The vortex configuration for the cone-cylinder became asymmetric at an angle of attack of  $22^\circ$ ; whereas the vortex wake for the triangular wing remained symmetric to an angle of attack about  $2^\circ$  or  $3^\circ$  greater. For

---

<sup>1</sup>It should be noted that the datum point for model 5-D ( $8^\circ$  apex angle cone-cylinder) does not fall on the correlation curve. The reason for this deviation will be discussed in a later section.

---

CONFIDENTIAL

this latter model the wake became asymmetric and unsteady at about the same instant without the appearance of the usual steady asymmetric vortex configuration. Although the angle of attack at which this occurred ( $25^\circ$ ) was very close to the angle of attack at which unsteadiness was first observed ( $26^\circ$ ) for the cone-cylinder model, the apparent agreement between the two results must be viewed with a certain amount of skepticism because the flow about the triangular-wing model may have been affected by the proximity of the tunnel normal shock wave. The unsteady normal shock wave moved upstream to the base of the triangular-plan-form wing model at an angle of attack of about  $25\text{--}1/2^\circ$  and could have caused the unsteadiness which was observed. It must be noted that for the other models tested interference from the normal shock wave did not occur.

In order to investigate further the effect of the axial rate of growth of the body cross-sectional area, a number of simple nonconical bodies were tested. These bodies included cusped nose shapes (models 11-B and 12-B), blunt nose shapes (models 8-B, 9-B, and 10-B), parabolic-arc bodies (models 19 and 20), and a circular-arc ogive (model 7-A). Correlation of the test results for these nonconical noses (fig. 4(b)) was made on the basis of nose fineness ratio rather than nose apex angle, because the latter did not appear to be the proper parameter to correlate the data for the blunt and the cusped nose shapes. Nevertheless, comparison of these results with the correlation curve for the conical-nosed models yields information as to the effect of nose profile. Two results are evident from this comparison. First, for nose shapes with apex angles less than that of a cone of the same fineness ratio, the angle of attack at which the vortex flow became unsteady was approximately the same as that for the "equivalent cone."<sup>2</sup> This result was evidenced in the data obtained with two similarly shaped noses (models 11-B and 12-B) which were more slender near their tips than the equivalent cones. The tips of these two models had theoretical semiapex angles of  $0^\circ$ , and the profiles were the theoretical nose profiles for minimum wave drag for a given volume and base diameter (ref. 6). These profiles differed only in their volumes, or fineness ratios, model 11-B having a fineness ratio 3 nose and model 12-B having a fineness ratio 6 nose. For the fineness ratio 6 nose shape, the angle of attack at which unsteadiness in the crossflow occurred was the same as that for the equivalent cone. For the fineness ratio 3 nose shape, the angle-of-attack range was not great enough to obtain unsteady wake flow. Nevertheless, a study of the vapor-screen photographs of the wake indicated that wake unsteadiness would probably have occurred at about the same angle of attack as for the equivalent cone. The angle of attack at which unsteady wake flow occurred for model 20, when plotted with the nose fineness ratio based on a nose length which included the spike, agreed with the cone correlation, as did the results for the cusped nose shapes. The second result obtained from the data of figure 4(b) was

---

<sup>2</sup>Hereinafter, the cone with a fineness ratio the same as that of the subject nose will be referred to as the "equivalent cone."

---

that for nose shapes which had apex angles greater than those of their equivalent cones (such as blunt-nosed shapes and circular-arc or parabolic-arc profiles); the angle of attack at which the vortex flow became unsteady was greater than that for the equivalent cone. This second result was evidenced by the data obtained from the tests with models 7-A and 19, circular-arc and parabolic-arc noses, respectively, where both the asymmetry and the unsteadiness in the wake occurred at larger angles of attack than for the equivalent cones. The results obtained for models 8-B, 9-B, and 10-B ( $3/4$ -power,  $1/4$ -power, and blunt Haack noses, respectively) showed that the wake flow was both symmetric and steady throughout the available angle-of-attack and Reynolds number ranges. On the other hand, the wake flow for the equivalent cone (model 2-B) became asymmetric at an angle of attack of about  $30^\circ$  and became unsteady for the highest Reynolds number at an angle of attack of about  $33^\circ$ .

The foregoing results have shown that expansion of the forebody in the vicinity of the body apex is an important geometric parameter, but not necessarily the only factor which determines the nature of the wake vortex configuration.

Expansion of the afterbody.- The effect of an expanding afterbody on the angle of attack at which the crossflow wake first becomes unsteady is of interest for application to configurations where a rearward center-of-pressure position is achieved by the use of either a conical afterbody (e.g., ref. 7) or triangular-plan-form wings of low aspect ratio. It has been shown that, for conical noses, the larger the axial rate of increase in cross-sectional area, the greater the angle of attack at which unsteady crossflow in the wake first occurs. Therefore, it was expected that a similar, although smaller, effect might be obtained if, for a given nose shape, various rates of afterbody expansion were used. Since expansion of the afterbody with distance from the body nose may be simply accomplished by the use of conical afterbodies, or by the addition of low-aspect-ratio, triangular-plan-form wings to a model, tests were made using both methods of expansion. The models with conical afterbodies consisted of a  $33\text{-}1/3$ -caliber ogival nose in combination with three afterbodies (models 7-A, 7-E, and 7-F) in which the conical expansion angle of the afterbody varied from  $0^\circ$  to  $8^\circ$  as shown in figure 2(a). The results of the tests with these bodies of revolution indicated that expanding the afterbody had little effect on the wake vortex configuration. In fact, for all three of the tests the angles of attack at which unsteady wake flow first occurred were within about  $\pm 1^\circ$  of each other. (This is approximately the uncertainty in the test results.)

The effect of afterbody expansion utilizing low-aspect-ratio, triangular-plan-form wings in combination with a cylindrical afterbody was investigated with models 13 and 14, the former having a conical nose and the latter an ogival nose. Vapor-screen photographs obtained for these two models with semiapex angle of the wings,  $\lambda$ , equal to  $4^\circ$  are



shown in figure 5.<sup>3</sup> These photographs show the wake vortex patterns at three longitudinal stations: one near the juncture of the wing leading edge and the body, the second about midway along the wing root chord, and the third at the trailing edge of the wing. The pictures for the most forward stations show that the symmetric pair for the ogival-nosed model and the asymmetric configuration for the conical-nosed model were established ahead of the wings on the noses of the models. The sequence of photographs for the conical-nosed model indicates that the asymmetric structure of the vortex pattern established on the nose remained asymmetric at the downstream stations in spite of the presence of the wings. From a consideration of these results and the results with the conical afterbodies, it appears that once a given vortex pattern is established on the nose of a body, expansion of the afterbody has little influence on the symmetry of the wake vortex pattern.

#### The Effect of Body Cross-Sectional Asymmetry

Consideration of two-dimensional-flow phenomena indicates that the nature of the flow within the crossflow wake depends upon the manner in which the crossflow separates from the body surface. Also, since asymmetry of the body cross section (relative to the oncoming crossflow) can cause asymmetric separation in the crossflow plane, it was reasoned that control of both the symmetry and steadiness of the flow might be achieved by artificially fixing the crossflow separation lines along each side of the body. In order to establish separation and to investigate the effects of both symmetric and asymmetric separation on the wake vortex pattern, sharp-edged separation strips were installed along the entire length of an  $8^\circ$  cone-cylinder (model 16) as shown in figure 2(c). Both the angle of attack and the angle of roll could be remotely controlled so that asymmetric separation could be induced at any angle of attack. Vapor-screen photographs with the model rotated to a position where the separation strips were perpendicular to the oncoming crossflow are shown in figure 6(a) for three angles of attack. With this symmetric orientation of the separation strips, the wake vortex pattern remained symmetric and stable as the angle of attack was increased from  $0^\circ$  to about  $23^\circ$ . For angles of attack between  $23^\circ$  and about  $26^\circ$ , the vortex pattern was still steady but asymmetric. Above an angle of attack of about  $26^\circ$  the wake flow became aperiodically unsteady. Comparison of the lowest angle of attack for unsteady wake flow for this model with the correlation curve of figure 4(a) indicates that symmetrically disposed separation strips do not appreciably affect the angle of attack at which unsteady wake flow first occurs. In fact, this comparison shows that the effect of separation strips was equivalent to increasing the apex angle from  $8^\circ$  to about  $12^\circ$ . The greater part of

---

<sup>3</sup>These photographs were taken with a movie camera mounted in the air stream behind the model and above the chord plane of the wing.

---

this increase in the effective apex angle probably resulted from the actual increase in the included angle of the separation strips at the tip of the cone, as shown in the detail sketch of figure 2(c).

As was expected, varying the roll angle,  $\Phi$ , of model 16 (which was equivalent to introducing a small sideslip angle) varied the wake vortex configuration. At an angle of attack of  $26^\circ$ , where the vortex wake was unsteady with the strips oriented at  $90^\circ$  to the oncoming crossflow, rolling the model only a small amount (about  $1/2^\circ$ ) was sufficient to stabilize the wake flow. Rolling the model to a little greater angle (about  $7^\circ$ ) was sufficient to produce an asymmetric pattern (fig. 6(b)) which remained steady throughout the available angle-of-attack range ( $0^\circ$  to about  $30^\circ$ ) and within the available Reynolds number range. No wake unsteadiness was found for angles of roll between  $7^\circ$  and about  $45^\circ$ . However, for angles of roll of the order of  $45^\circ$  and greater, the separation strips were ineffective in controlling the position of crossflow separation, and, at angles of attack as low as  $20^\circ$ , violent wake fluctuations occurred for certain combinations of angle of attack and angle of roll. Thus, when the strips were oriented at an angle of roll of  $90^\circ$  simulating a splitter plate between the vortices on the lee side of the model, the angle of attack at which wake unsteadiness occurred was about the same as for the basic cone-cylinder model. Through the use of model 15 with wing semiapex angles of  $6^\circ$  and  $10^\circ$ , the size of the splitter plate was increased so that at any axial position the splitter plate extended farther into the lee side wake.<sup>4</sup> The results obtained with model 15 showed that only with the  $10^\circ$  semiapex angle splitter plate was the angle of attack for unsteady wake flow increased. For the  $6^\circ$  semiapex angle splitter plate, the angle of attack at which the wake became unsteady ( $17^\circ$ ) was the same as for the cone-cylinder model. For the  $10^\circ$  semiapex angle splitter plate, the occurrence of unsteady wake flow was delayed to an angle of attack of about  $31^\circ$ . It is apparent that the angle-of-attack range for stable wake flow can be increased through the use of splitter plates.

It is also of interest to note that the results obtained by varying the roll angle of model 15 (triangular-plan-form wing model of very low aspect ratio with wing apex at the tip of the body) were similar to the results obtained with model 16 in that small changes in roll angle were sufficient to affect the symmetry of the wake vortex pattern. It should be pointed out that the variations in vortex pattern with small changes in roll angle, similar to those which have been observed for models 15 and 16, might give rise to appreciable rolling moments and guidance difficulties for full-scale vehicles with noncircular cross sections.

The results of the tests with separation strips and the tests with triangular-plan-form wings of very low aspect ratio have indicated that

---

<sup>4</sup>In reference 8 the unsteady wake flow from a two-dimensional cylinder was stabilized by the addition of a splitter plate.

---

a vortex wake which was both symmetric and steady could not be maintained throughout the angle-of-attack range even when the lines of crossflow separation were established along the entire body length in a symmetrical manner. Nevertheless, the results did indicate that it might be possible to maintain steady wake flow to large angles of attack by purposely introducing an asymmetry in the body, although in doing so an asymmetric vortex flow in the low angle-of-attack range would have to be accepted. Such a vortex flow might be accomplished by simply fixing a single separation line near the tip of the body. Therefore, an  $8^\circ$  cone-cylinder was tested with a single small separation fin on one side of its tip (essentially an asymmetric tip section on the cone), as shown on model 17 in figure 2(c). Although unstable wake flow was observed for a smooth cone with an  $8^\circ$  apex angle (fig. 4(a)), no wake unsteadiness was found for model 17 throughout the available range of angles of attack and Reynolds number. Typical vapor-screen photographs of the wake for three angles of attack and two Reynolds numbers are presented in figure 7 and show the asymmetric structure of the wake vortex pattern for the tests with the small fin oriented perpendicular to the oncoming crossflow. The results for this model with the large tip asymmetry provide an explanation for the previously observed results for the  $8^\circ$  cone-cylinder (model 5-D) in figure 4(a). Careful inspection of model 5-D showed that even though considerable care had been taken in the construction of the model a minute rotational asymmetry (subsequently revealed by 100X magnification of the model tip) had been inadvertently added to the first few hundredths of an inch of its tip. The vapor-screen pictures in figure 8 for this model at one angle of attack and three attitudes in roll show the variations of the wake vortex pattern which resulted from the small tip asymmetry. Thus, it appears that the asymmetry of the model caused variations in the symmetry of the vortex pattern as the model was rotated to various attitudes in roll (fig. 8) and inhibited the occurrence of unsteady wake flow (fig. 4(a)).

Summarizing the results of the tests with separation strips and very low-aspect-ratio, triangular-plan-form wings with regard to wake unsteadiness, it appears that a small separation strip, or tip asymmetry, such as the one used on model 17, is the most effective means of inhibiting unsteadiness in the crossflow. In order to investigate the effectiveness of such strips on other nose shapes, a small fin similar to that used on the  $8^\circ$  cone-cylinder was attached to the nose of a fineness ratio 5 tangent ogive with a cylindrical afterbody (model 18). Results of the tests with this model showed that, although at small angles of attack the fin caused the wake vortices to be asymmetric instead of symmetric, the fin had little effect on the pattern at large angles of attack or on the angle of attack at which unsteadiness in the crossflow occurred. Similar results were obtained from a second test of model 18 with the span and root chord of the small triangular-plan-form fin doubled. Hence, even though the small separation strip, or tip asymmetry, at the tip of a slender nose (such as the  $8^\circ$  cone) may inhibit the onset of unsteadiness in the crossflow as the angle of attack is increased,

this device may not achieve the same results for other more blunt nose shapes (such as model 18).

### Reynolds Number Effects

The effect of Reynolds number on the crossflow vortex pattern was investigated for most of the models tested. It was found that, in general, an increase in Reynolds number was accompanied by a decrease in the angle of attack at which asymmetry, and subsequent unsteadiness, in the vortex pattern was observed. (See, e.g., the occurrence of asymmetry in the vortex patterns shown in fig. 9.) However, for a few of the more blunt models, it appeared that the effect of body shape overshadowed any effect of Reynolds number. For example, the results of the tests with the 30° cone-cylinder (model 1-A) indicated that the effect of Reynolds number on the behavior of the vortices was negligible for the range of Reynolds numbers available in the present investigation.

### Effects of Vortex Configuration on Body Forces

Changes in the crossflow wake characteristics for a body of revolution at an angle of attack might be expected to be accompanied by variations of the body normal force and possibly the pitching moment. Therefore, measurements of the lift, drag, and pitching moment were made on the 5° cone (model 6-E) to investigate this possibility. It was found that for this model the desired change in the wake vortex configuration from asymmetric to symmetric could be obtained by modifying the cone-tip shape.<sup>5</sup> The results of the tests indicated identical curves of lift, drag, pitching moment, and center of pressure for both wake conditions. Hence, it was concluded that for the test conditions of the present investigation, these force characteristics were essentially independent of variations in the steady configuration of the crossflow vortices, even though there obviously were some changes in the local pressure distributions. These variations in local pressure distribution with changes in the vortex pattern might cause more of an effect on side forces and yawing moments (not measured in the present investigation) than on the lift, drag, and pitching moments. In fact, in reference 9 results of a series of pressure-distribution measurements made on a body of revolution at large angles of attack indicated a large effect of the crossflow asymmetry on the side forces. Large local side forces were found but, because of the fact that the magnitudes of the local side forces varied from large positive to large negative values along the body, the net side forces were rather small. The axial

---

<sup>5</sup>The modification to the model consisted of removing 1/4 inch from the cone apex and forming a hemispherical tip in place of the sharp point.

---

variation of the local side forces gave rise to appreciable yawing moments. These yawing moments varied in sign as well as magnitude when the angle of attack was increased from  $0^\circ$  to about  $36^\circ$ .

#### CONCLUDING REMARKS

The results of the present investigation have brought out certain salient facts which may be important to the designer of aircraft required to fly at large angles of attack at supersonic speeds. Since an unsteady vortex wake in the lee of a body may lead to undesirable control characteristics and to tail buffeting, the factors which affect the behavior of the vortices are important. The results of the present investigation indicate that both body shape and Reynolds number affect the vortex configuration. Of the various body-shape variables, it appears that the shape of the nose has the greatest influence on the behavior of the vortices. If the designer has to select one of several nose shapes, which may be equally acceptable from other considerations, then, to minimize adverse effects of the body vortex wake, the nose shapes of lower fineness ratio and more blunt contour appear desirable. The addition of external longitudinal fairings (tunnels) or other protuberances, which result in a noncircular cross section, affects the configuration of body vortices and may lead to undesirable rolling moments.

Ames Aeronautical Laboratory  
National Advisory Committee for Aeronautics  
Moffett Field, Calif., Sept. 17, 1953

#### REFERENCES

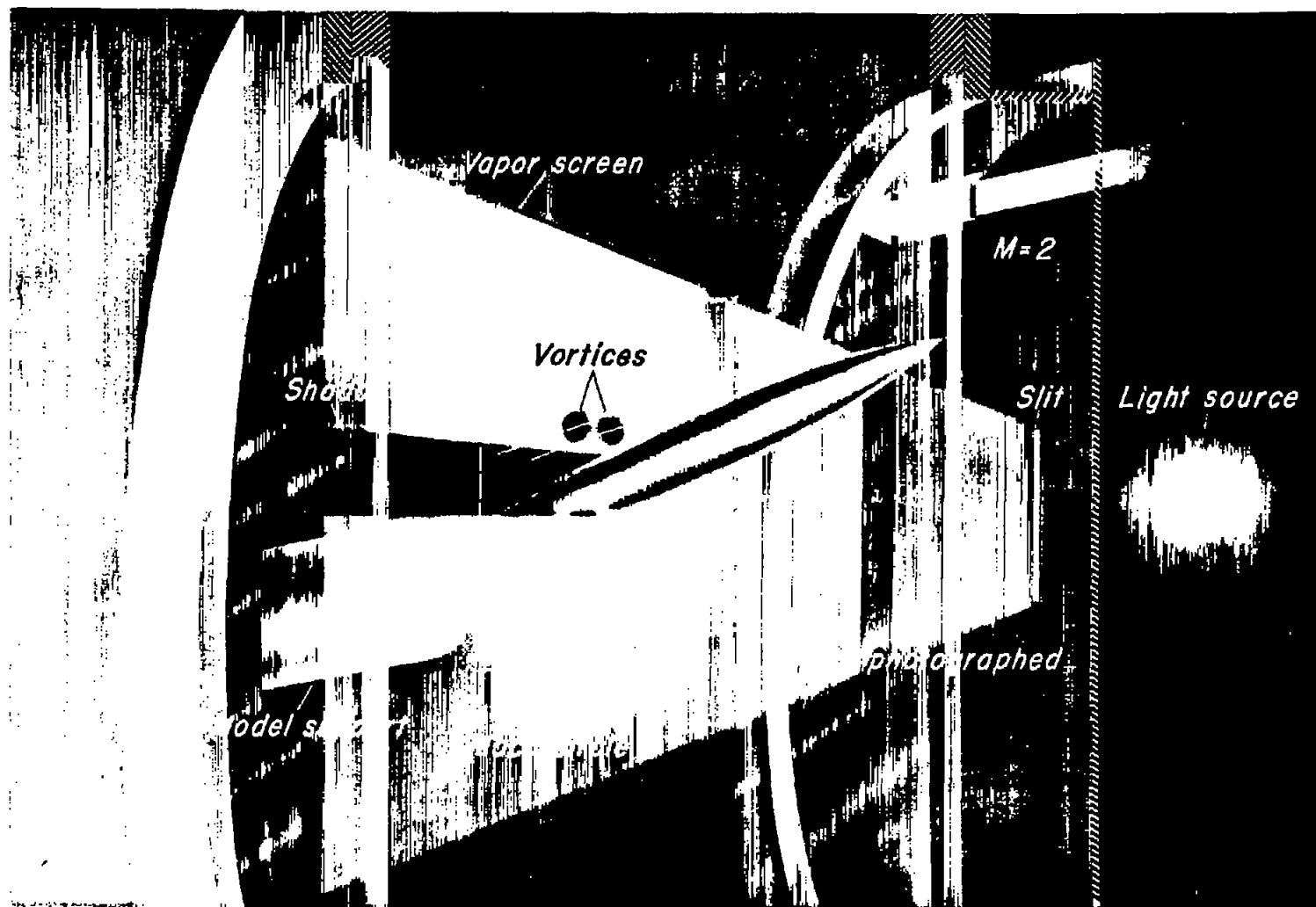
1. Allen, H. Julian, and Perkins, Edward W.: Characteristics of Flow Over Inclined Bodies of Revolution. NACA RM A50LO7, 1951.
2. Gowen, Forrest E.: Buffeting of a Vertical Tail on an Inclined Body at Supersonic Mach Numbers. NACA RM A53A09, 1953.
3. Seiff, Alvin, Sandahl, Carl A., Chapman, Dean R., Perkins, Edward W., and Gowen, Forrest E.: Aerodynamic Characteristics of Bodies at Supersonic Speeds - A Collection of Three Papers. NACA RM A51J25, 1951.
4. Mead, Merrill H.: Observations of Unsteady Flow Phenomena for an Inclined Body Fitted With Stabilizing Fins. NACA RM A51K05, 1952.

5. Moore, Franklin K.: Laminar Boundary Layer on Cone in Supersonic Flow at Large Angle of Attack. NACA TN 2844, 1952.
6. Haack, W.: Projectile Forms for Minimum Wave Resistance. (Translation) Douglas Aircraft Co., Inc., Rep. 288, 1946.
7. Ross, F. W., and Dorrance, W. H.: An Introduction to a Supersonic Body Developmental Study, University of Michigan. UMM-40, Dec. 1949.
8. Roshko, Anatol: On the Development of Turbulent Wakes from Vortex Streets. NACA TN 2913, 1953.
9. Cooper, Morton, Gapcynski, John P., Hasel, Lowell E.: A Pressure-Distribution Investigation of a Fineness-Ratio-12.2 Parabolic Body of Revolution (NACA RM-10) at  $M = 1.59$  and Angles of Attack up to  $36^\circ$ . NACA RM L52G14a, 1952.

[REDACTED]

CONFIDENTIAL

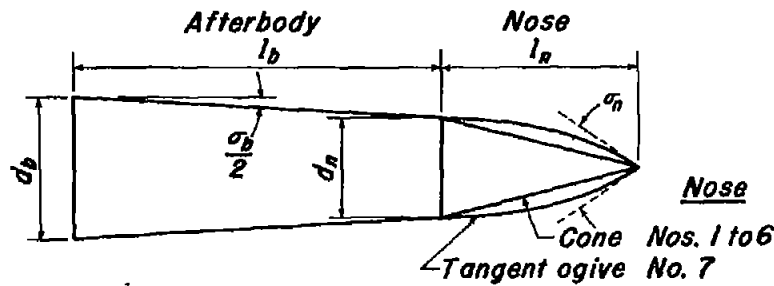
[REDACTED]



A-18338

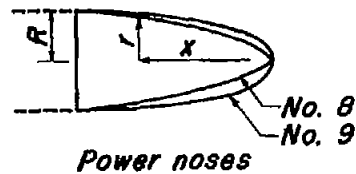
Figure 1.- Schematic diagram of vapor-screen apparatus showing vortices from a lifting body of revolution.





$$\frac{r}{R} = \left(\frac{x}{l_n}\right)^n$$

Nose	n
8	$\frac{1}{4}$
9	$\frac{1}{2}$

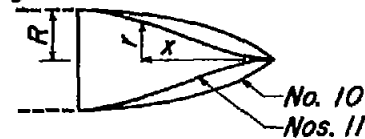


Power noses

$$r = \frac{R}{\sqrt{\pi}} \sqrt{\xi - \frac{1}{2} \sin 2\xi + c \sin^3 \xi}$$

$$\xi = \cos^{-1} \left(1 - \frac{2x}{l_n}\right)$$

Nose	c
10	$-\frac{3}{8}$
11, 12	$\frac{1}{8}$



Haack noses

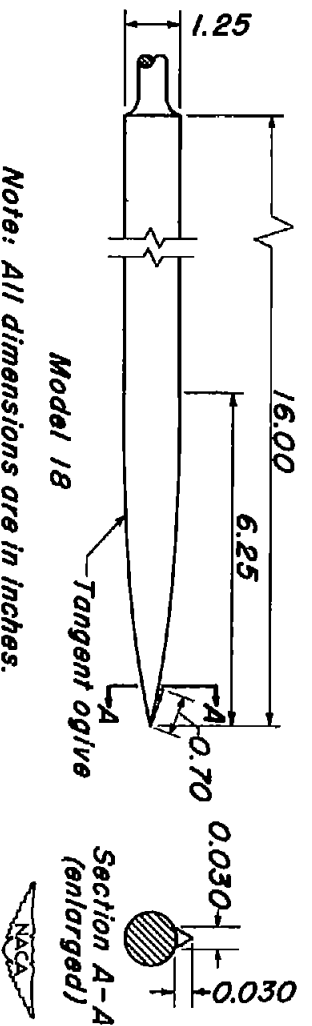
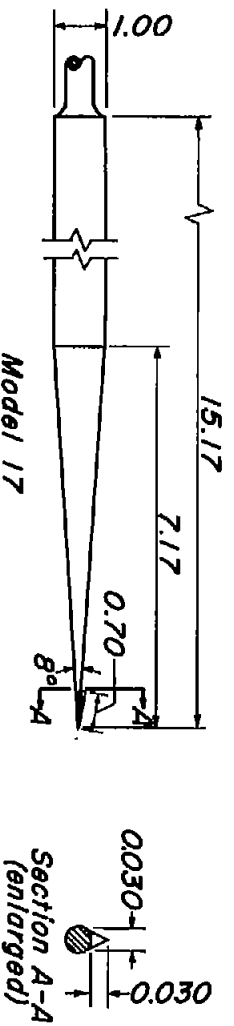
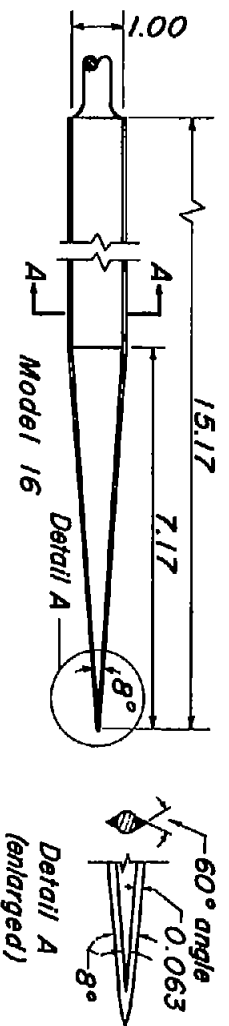
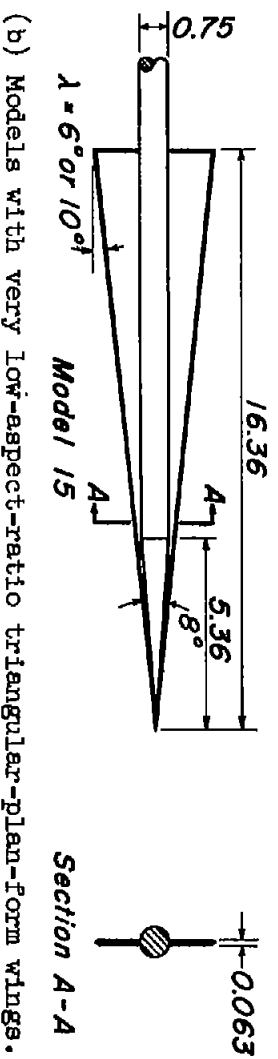
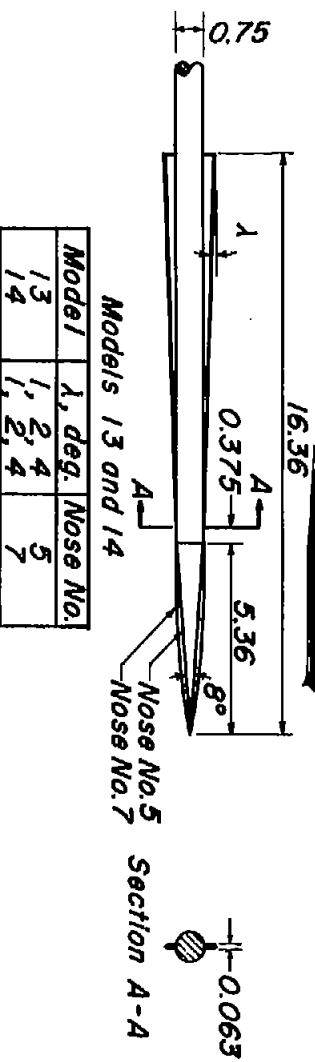
Model	$l_n/d_n$	$\sigma_n$ deg.	Afterbody		$l_b$ in.	$d_b$ in.
			type	$\sigma_b$ , deg.		
1-A	1.87	30.0	Cyl.	0	7.00	0.75
2-B	3.00	19.0			7.00	1.75
3-C	5.00	11.5			16.00	1.25
4-B	6.75	8.5			7.00	1.75
5-D	7.15	8.0			8.00	1.00
5-F	7.15	8.0	Conical	8.0	9.92	2.13
6-A	11.45	5.0	Cyl.	0	7.00	0.75
7-A	5.75	19.7				0.75
8-B	3	180.0				1.75
9-B						
10-B						
11-B		0 (theo.)				
12-B	6	0 (theo.)				
6-E*	11.45	5.0	Conical	5.0	7.66	1.34
7-E	5.75	19.7		5.0	7.66	1.34
7-F	5.75	19.7		8.0	9.92	2.13

\*Note: One 5° cone was modified by removing  $\frac{1}{4}$  inch from its apex and forming a hemispherical tip in place of the sharp point.



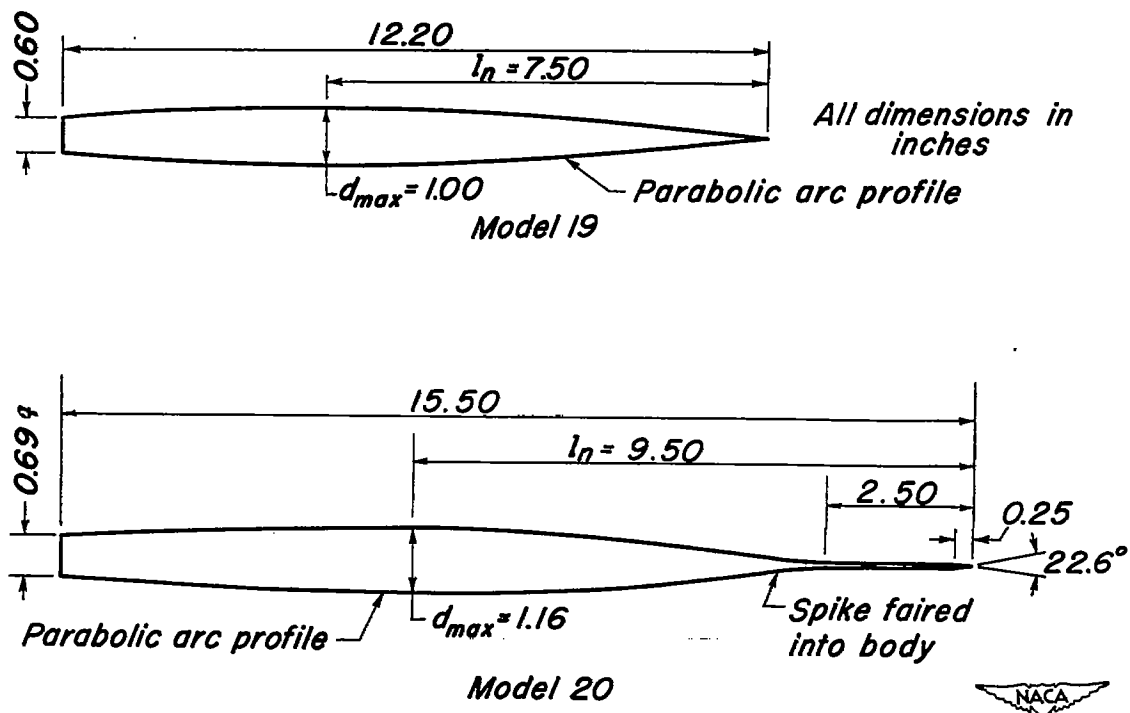
(a) Models with conical and cylindrical afterbodies.

Figure 2.- Sketches of models.



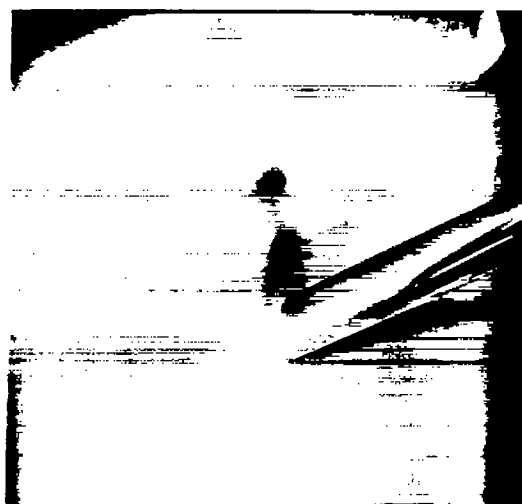
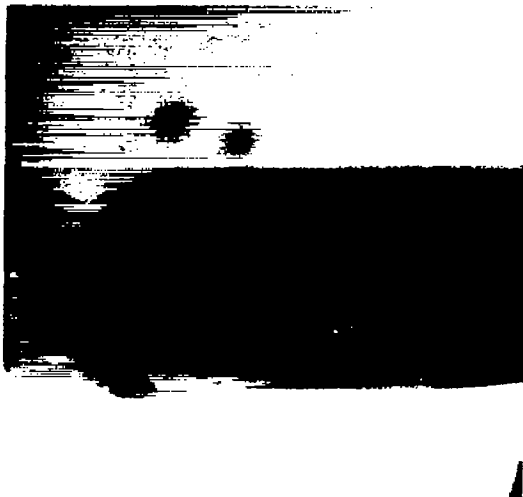
Note: All dimensions are in inches.  
Edges of all separation strips are sharp.

(c) Models with separation strips.  
Figure 2.- Continued.



(d) Parabolic-arc models.

Figure 2.- Concluded.

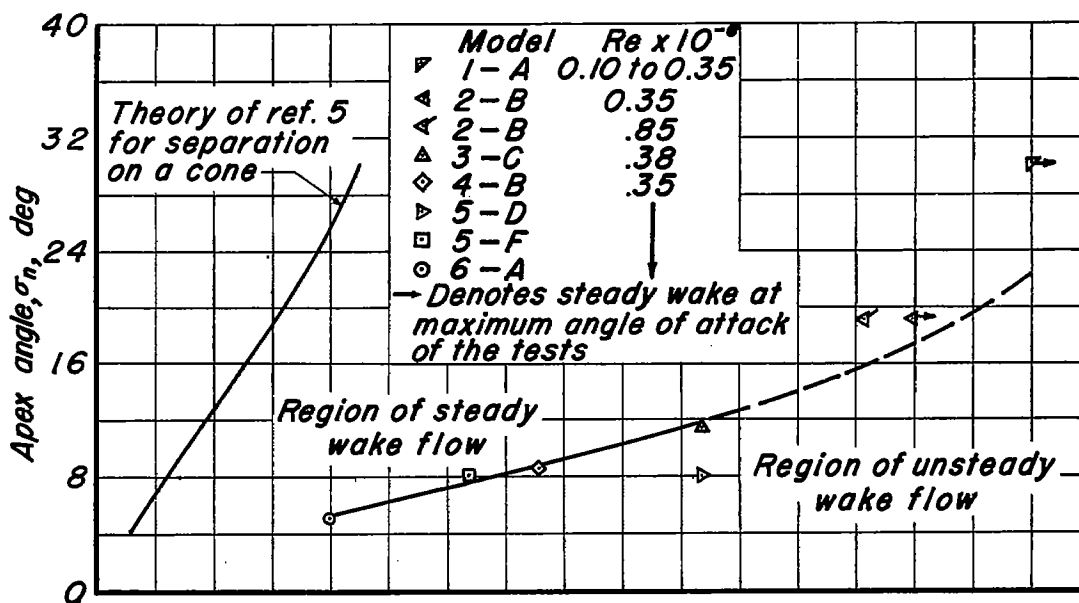


A-18339

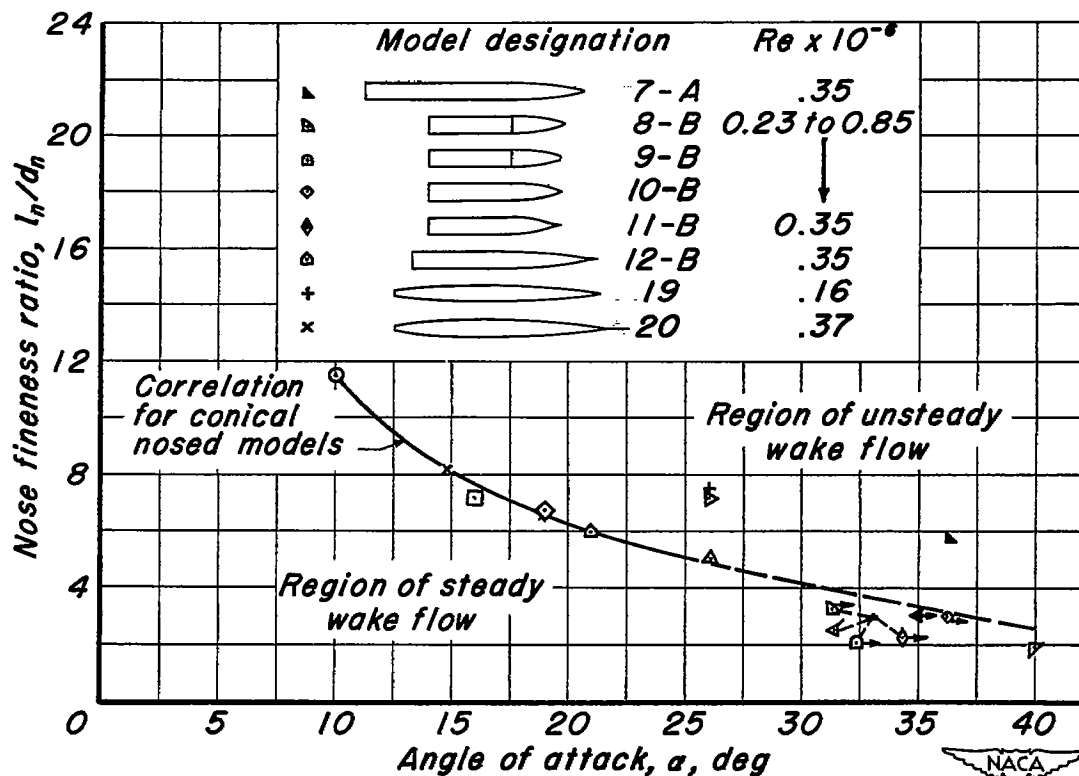
(a) Typical symmetric  
vortex patterns.

(b) Typical asymmetric  
vortex patterns.

Figure 3.- Examples of the types of steady vortex patterns observed in  
the wakes of bodies of revolution.

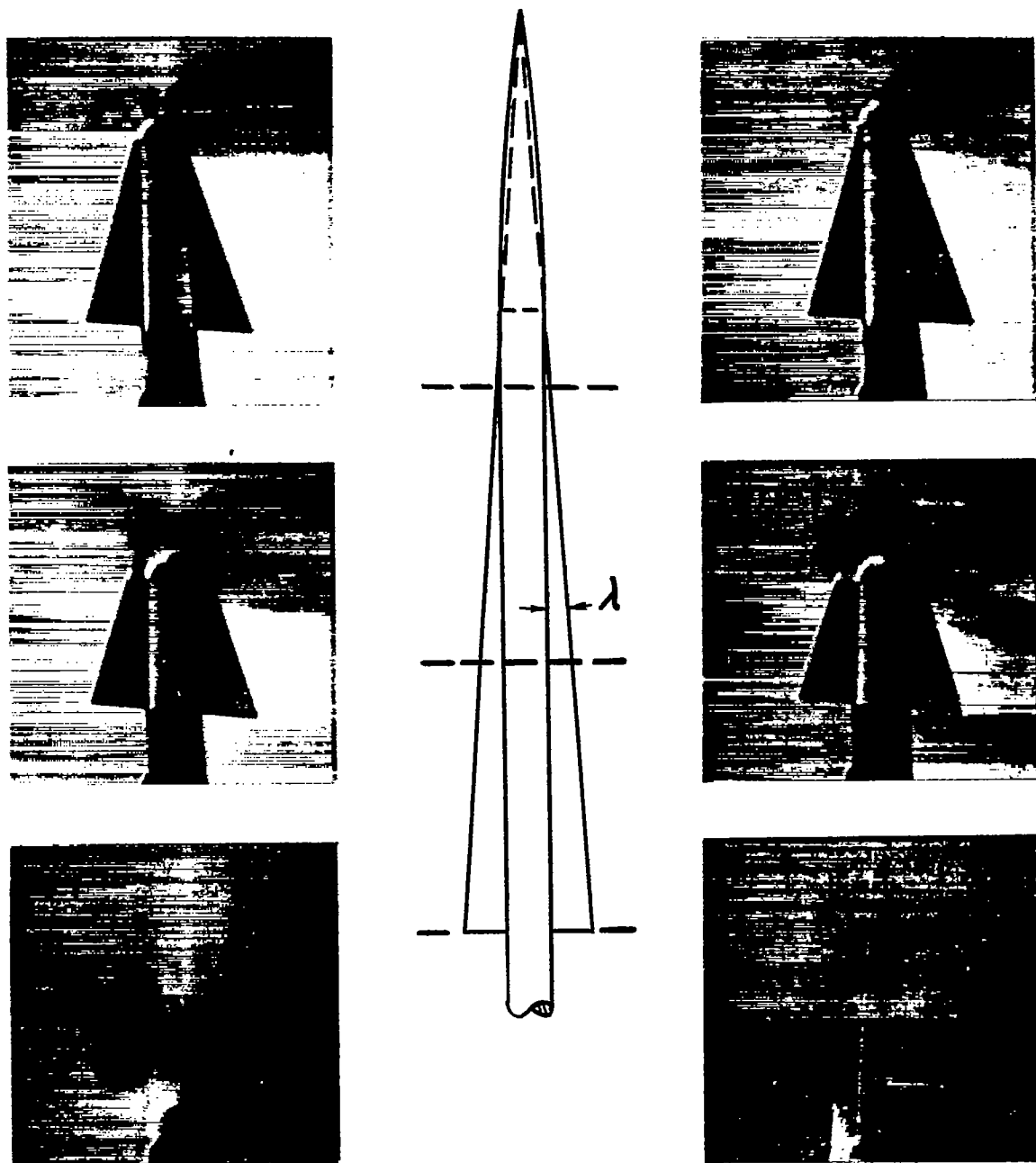


(a) Effect of apex angle for conical noses.



(b) Effect of nose fineness ratio.

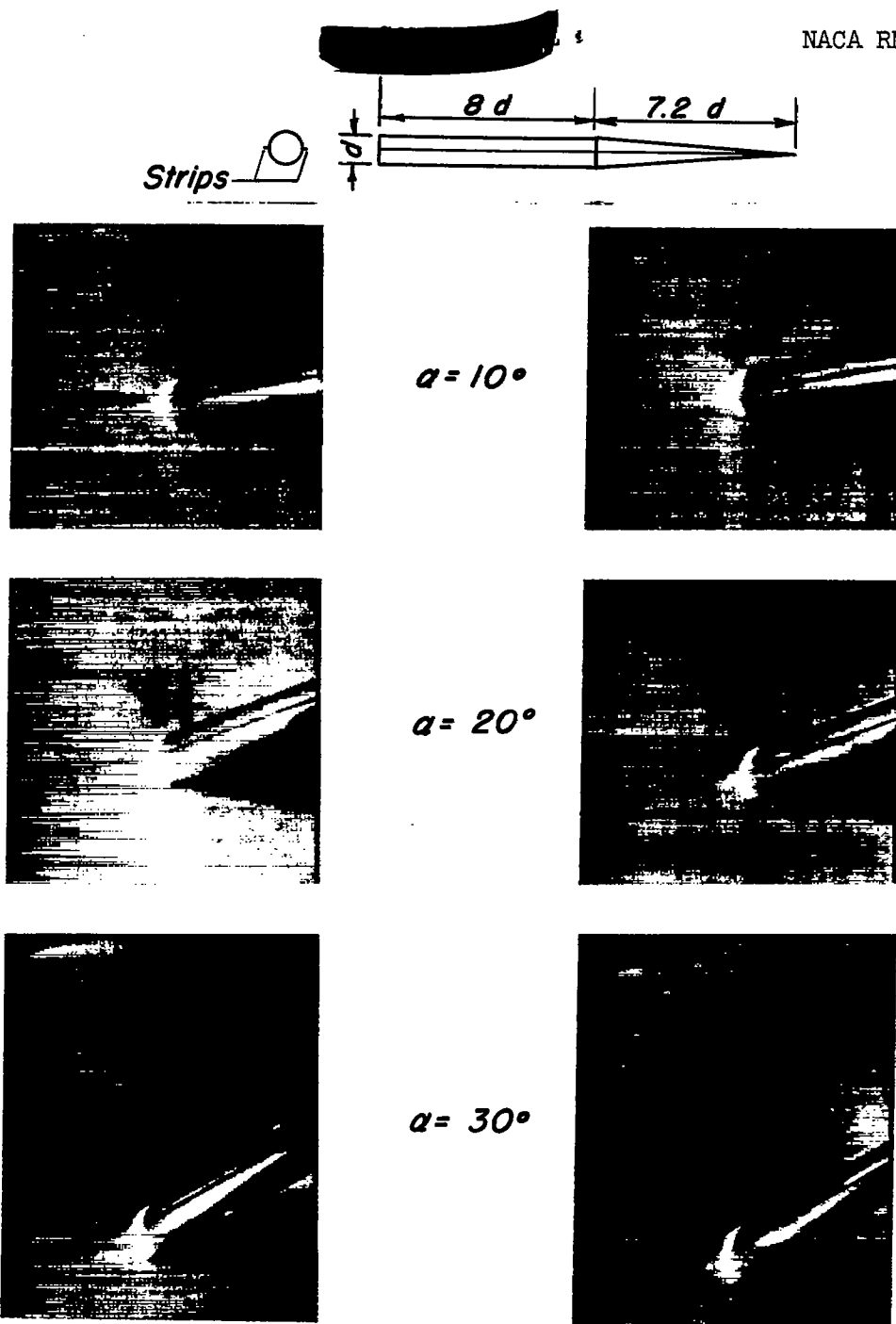
Figure 4.- Effects of apex angle and nose fineness ratio on the angle of attack at which unsteadiness in the crossflow occurs.



(a) Ogival-nosed model  
(model 14).

(b) Conical-nosed model  
(model 13).

Figure 5.- Vapor-screen photographs showing the wakes of two models  
with large separation strips ( $\alpha=17^\circ$ ,  $\phi=0^\circ$ ,  $\lambda=4^\circ$ ).

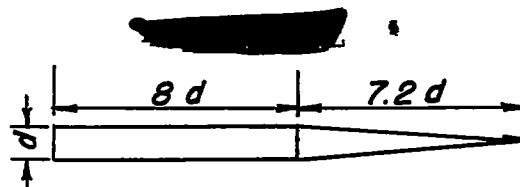


A-18341

(a) Separation strips  
horizontal ( $\phi=0$ ).

(b) Model rotated  
( $\phi=7^\circ$ ).

Figure 6.- Vapor-screen photographs showing the effect of roll on the vortex configuration in the wake of an  $8^\circ$  cone-cylinder (model 16) with separation strips.



$\alpha = 10^\circ$



$\alpha = 20^\circ$



$\alpha = 30^\circ$



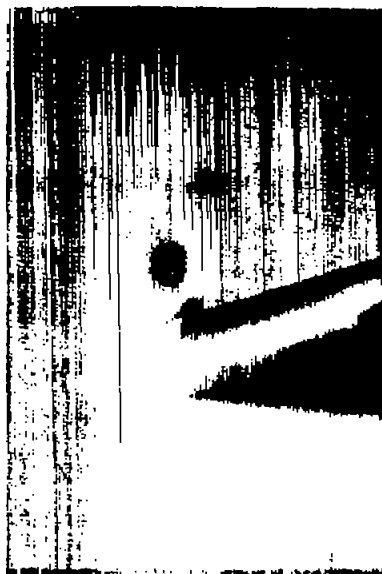
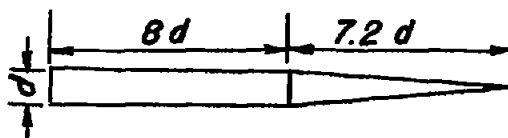
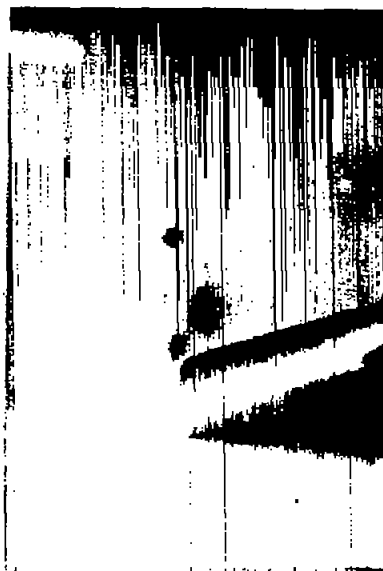
A-18342

(a)  $Re = 0.1 \times 10^6$

(b)  $Re = 0.5 \times 10^6$

Figure 7.- Vapor-screen photographs of the wake of model 17 ( $\sigma_n = 8^\circ$ ) for various angles of attack and two Reynolds numbers.

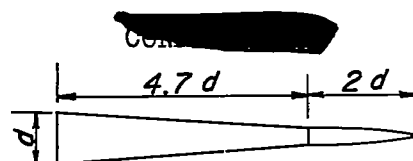


Roll angle =  $0^\circ$ Roll angle =  $67^\circ$ 

A-18343

Roll angle =  $139^\circ$ 

Figure 8.- Vapor-screen photographs showing the effect on the vortex wake of a minute rotational asymmetry in the tip of an  $8^\circ$  cone-cylinder (model 5-D). ( $\alpha=15^\circ$ ;  $Re=0.50 \times 10^6$ )


 $\alpha = 25^\circ$ 

 $\alpha = 29^\circ$ 

 $\alpha = 33^\circ$ 


A-18344

(a)  $Re = 0.14 \times 10^6$ (b)  $Re = 0.69 \times 10^6$ 

Figure 9.- Vapor-screen photographs showing the effect of Reynolds number on the vortex pattern for an ogival nose with an expanding afterbody (model 7-F).